Journal of Visualization, Vol. 8, No. 3 (2005)245-252

4D-PTV

Measurements of an Impinged Jet with a Dynamic 3D-PTV

Hwang, T. G.*[1], Doh, D. H.*[2] and Okamoto, K.*[3]

*1 Graduate School, Korea Maritime University, Busan, Korea. E-mail: andrew@bada.hhu.ac.kr
*2 Division of Mechanical and Information Engineering, Korea Maritime University, Youngdo-ku, Dongsam-dong, Busan, 606-791, Korea.
*3 The Univ. of Tokyo, Dept. of Quantum Eng. & Systems Science, Hongo, Bunkyo-ku, Tokyo, Japan.

Received 1 October 2004
Revised 28 March 2005

Abstract : 4D-PTV system was constructed. The measurement system consists of three high-speed high-definition cameras (1k x 1k, 2000 fps), Nd-Yag laser (2000 Hz) and a host computer. The GA-3D-PTV algorithm was used for completing the measurement system. The 4D-PTV is capable of probing the spatial distribution of velocity vectors of the flow field overcoming the temporal resolution of the characteristic turbulence length scales of the measured flow fields. A horizontal impinged jet flow (H/D = 7) was measured. The Reynolds number is about 33,000. Spatial temporal evolution of the jet flow was examined and physical properties such as spatial distributions of vorticity and turbulent kinetic energy were obtained with the constructed system.

Keywords: : 4D-PTV, GA-3D-PTV algorithm, Impinged Jet, Vortex Ring.

1. Introduction

Submerged impinged jets have received substantially more attention in the literature than have impinged free liquid jets. The velocity gradient near the stagnation point had been shown by many pervious analytical and experimental investigations to be an important parameter in stagnation heat transfer (Sibulkin, 1952; Burmeister, 1983). Several related factors, including the jet exit velocity profile, and stagnation region radial velocity gradient have been proposed to be of importance in governing the heat transfer under an impinged jet (Vader et al., 1991). Olsson and Turkdongan (1966) investigated experimentally the radial flow field of an impinged liquid jet with pointwise measurement results. Gardon et al. (1965) discovered how the turbulent flow can effect heat transfer when a free jet was impinged on the surface of a plate. Kataoka et al. (1986) showed that period of vortex could change the effect of heat transfer at the impinged plate. Most of the results obtained by previous researches were based on pointwise measurement techniques such as, Hot wire and LDV. No matter how the numerical results are accurate, the results should be proved by the results obtained from an experiment because the flow fields are too complicate to be modeled more accurately. In order to attain accurate analysis on the impinged jet, it is necessary to know vortical structures of the jet. There have been some efforts to study the influence of the vortical structures of an impinged jet on heat transfer. Faggiani and Grassi (1990) studied the influences of the local and average heat transfer characteristics by studying the influence of flow structure on

transport with the results on large-scaled flow structures. Bae et al. (2001) investigated the influence of the impinged angles with 2-dimensional PIV technique. To make a complete analysis on the influences of the flow structures of the jet, 3-dimensional measurements are necessary. Nishino et al. (1996) carried out 3D-PTV measurement on an impinged jet and provided statistics of the turbulent properties near the stagnation region with two camera 3D-PTV system (Hagiwara et al., 2000). Since the number of instantaneous velocity vectors obtained was not so many, the structural analysis on the impinged jet couldn't be made. Recently, Nishino and Takahashi (2003) carried out a dynamic PIV measurement with high-frequency and high-definition camera (1k x 1k) and tried to find out the temporal evolution of flow structures. In order to attain more accurate analysis on the influences of the vortical structures of the jet onto the heat transfer of the heated plates, the number of instantaneous three-dimensional velocity vectors should be enough. Mass et al. (1993) could get more than 1000 instantaneous three-dimensional velocity vectors for three-dimensional channel flow with a three-camera arrangement. However, the flow field was restricted to the boundary region of a channel flow. In the mean while, Doh et al. (2002) obtained more than 98% of correct vectors from initial velocity vectors for a forced vortex flow field by introducing a genetic algorithm (GA) to the conventional 3D-PTV system. They took a consideration onto the disappearing particles' pairs between two image frames and reused those particles pairs for GA calculation to enhance the recovery ratio of correct vectors. They obtained more than 3000 instantaneous three-dimensional velocity vectors for the wake of a sphere with low resolution cameras (0.5K x 0.5K)(2004). The aim of this study is to construct a system called 4D-PTV system that improves the restrictions of the temporal and spatial resolutions of the conventional PIV system by revising their algorithm of the 3D-GA-PTV (2002, 2004) and by replacing the system with high-definition-high-speed cameras and a high-speed pulsed laser system, and to construct a database on an impinged jet.

2. Measurement System

2.1 Experimental Setup and Procedures

Figure 1 shows the experimental setup. The Reynolds number is about 33,000 with the nozzle diameter D = 20 mm. The distance between the flat plate and the nozzle is H/D = 7.

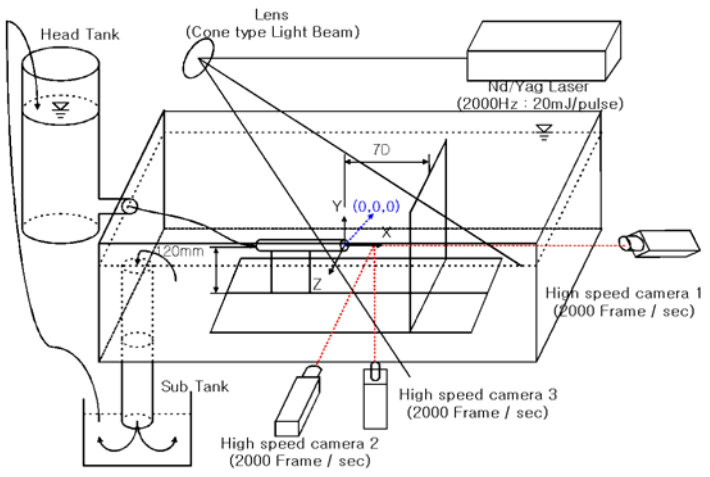

Fig. 1. 4D-PTV system for the impinged jet flow.

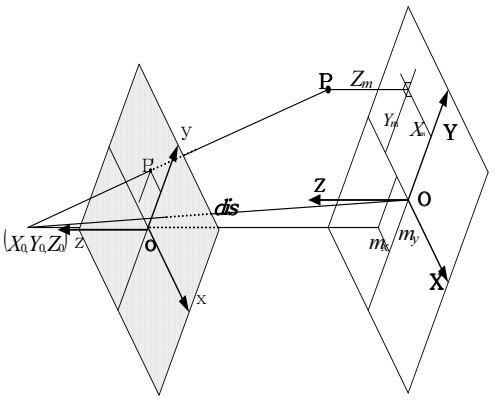

Fig. 2. Relations of camera parameters on the absolute and the photographical coordinates.

Three Photron Fast CAM APX (Max) cameras and Coherent Corona Laser (10 mJ, 2000 Hz) were used to overcome temporal and spatial resolution of the conventional 3D-PTV system. The image resolution of the camera is 1024 x 1024 pixel with 2000 fps. Using the camera, the

high-temporal and spatial resolution images could be captured. All hardware components of the system were synchronized for simultaneous image capturing. A multi-sectioned calculation algorithm used for the calculation of the GA-Based 3D-PTV algorithm (Doh et al., 2002, 2004) in order to save the calculation time. The size of the measurement region is 90 mm x 90 mm x 90 mm. The origin of the absolute coordinate (X = 0, Y = 0, Z = 0) for the impinged jet was defined at the end of nozzle's center.

For the measurement of 3D-PTV, camera calibration was carried out using a calibrator on which 42 landmarks were installed. The three-dimensional positions of these landmarks were measured by an optical system (BLN-C797) which has a precision of ±0.001 mm. The apertures of the three cameras were adjusted to focus on the whole landmarks' images in order not to take blurred particles' images. After completing the camera calibration and the construction of the flow field, tracer particles (diameter = 100 μm, specific gravity = 1.02) were put into the flow field for flow visualizations. The volume light illumination was used making fore-scattering for all three cameras in order to produce clear particles' images. The images captured by the three cameras were transferred to the host computer in which the centroids of the particles were calculated. In this study, the camera parameters and the three-dimensional vectors were obtained by the method GA-Based 3D-PTV algorithm (Doh et al., 2002, 2004).

2.2 4D-PTV System

To get the three-dimensional velocity vectors, camera parameters such as the exterior (the position and the orientations of the camera) and the interior parameters (the focal length, deviations of the principal point and the distortion coefficients of the camera lens) were obtained in advance. Next, three-dimensional position of each particle was calculated. Finally, three-dimensional velocity vectors were calculated. In this study, 10 parameters (6 exterior parameters: $dis, \alpha, \beta, \gamma, m_x, m_y$, 4 interior parameters: c_x, c_y, k_1, k_2) were obtained. (α, β, γ) represents the tilting angles of the axes of the photographic coordinates against the absolute axes. c_x and c_y are the focal distances for x and y components of the coordinate. Figure 2 shows a coordinate relation when the photographical axes had been set to parallel with the absolute coordinate by tilting with the angles (α, β, γ). (X, Y, Z) represents the absolute coordinate, and (x, y, z) the photographical coordinate of the objective point. The notation *dis* means the distance between the origin O (0, 0, 0) and the principal point (X_0, Y_0, Z_0) of the camera. The coordinate (X_m, Y_m, Z_m) represents the position of the point P when the camera coordinate is rotated with the tilting angles to make the collinear set in one line as shown in Fig. 2.

$$x - \Delta x = c_x \frac{X_m - m_x}{\sqrt{dis^2 - m_x^2 - m_y^2} - Z_m}, \quad y - \Delta y = c_y \frac{Y_m - m_y}{\sqrt{dis^2 - m_x^2 - m_y^2} - Z_m} \tag{1}$$

$$\Delta x = (x/r) \times \left(k_1 r^2 + k_2 r^4\right), \quad \Delta y = (x/r) \times \left(k_1 r^2 + k_2 r^4\right), \quad r = \sqrt{x^2 + y^2} \tag{2}$$

The m_x, m_y means the point at which the vector constructed with the camera principle point O (Xo, Yo, Zo) and the origin of the camera coordinate meets the X-Y plane of the absolute coordinate. Camera parameters were obtained by using the 42 landmarks based on Eq. (1), and the absolute coordinates of the particles' image were obtained by taking the transformation as Eq. (3) using the

$$\begin{bmatrix} X \\ Y \\ Z \end{bmatrix} = \mathrm{M}_M^{-1} \begin{bmatrix} X_m \\ Y_m \\ Z_m \end{bmatrix} \tag{3}$$

inverse matrix M_M^{-1} whose elements consisted of the parameters. Here, M_M is the matrix for the rotational transformation and (X_m, Y_m, Z_m) is expressed in the form of Eq. (4).

$$\mathrm{X}_m = \frac{x - \Delta x}{c_x} t + m_X, \; \mathrm{Y}_m = \frac{y - \Delta y}{c_y} t + m_y, \; \mathrm{Z}_m = \mathrm{d} - \mathrm{t}, \; \mathrm{d} = \sqrt{dis^2 - m_X^2 - m_y^2} \tag{4}$$

From the two camera (A, B) system, the three-dimensional position of the particle was obtained by

using the following Eq. (5).

$$\begin{bmatrix} X_P \\ Y_P \\ Z_P \end{bmatrix} = \frac{1}{2}\left\{ \begin{bmatrix} X_A \\ Y_A \\ Z_A \end{bmatrix} + \begin{bmatrix} X_B \\ Y_B \\ Z_B \end{bmatrix} \right\}$$

$$X_A = (a_{11}t + b_{11}, a_{12}t + b_{12}, a_{13}t + b_{13}),\ X_B = (a_{21}s + b_{21}, a_{22}s + b_{22}, a_{23}s + b_{23}) \quad (5)$$

Here, t and s were obtained by the least square method (LSM). In order to calculate the three-dimensional positions of particles, corresponding pairs the centroids of particles of the two sets of camera images should be discovered among many other particles. A genetic algorithm based 3D-PTV algorithm has been adopted to find the true corresponding pairs. Detailed calculation processes for finding the pairs and camera parameters can be referred to the references of Doh et al. (2002, 2004). Since the image data are large, a multi-section calculation method was introduced to save the calculation time in which the measured volume was divided into four districts.

3. Measurement Results

3.1 Transient Velocity Tracking

Figure 3 shows one of the instantaneous raw images captured by the camera 2 located as in Fig. 1. Figure 4 shows the instantaneous three-dimensional velocity vectors. The number of the instantaneous vectors obtained in one processing was about 10,000. Among these erroneous vectors are eliminated using the Tompson's Tau Method (Coleman & Steele, 1999) in which the correct vectors are only selected in a small volume that corresponds to the size of a virtual probe sensor. The number of vectors judged as correct ranged between 5000 and 6000. Figure 5 shows the ensemble grid vectors which were obtained from the correct vectors after eliminating the erroneous vectors using 2000 image frames. Figure 6 shows instantaneous vorticity distribution. The distribution represents the vorticity ($\omega = (\omega_x{}^2 + \omega_y{}^2 + \omega_z{}^2)^{1/2}$) at three YZ planes at x/D = 2.3, 3.5 and 5.1. It can be said that there exist ring vortexes along the axis of the jet, which can be explained by vorticity distribution on XY center plane as shown in Fig. 6.

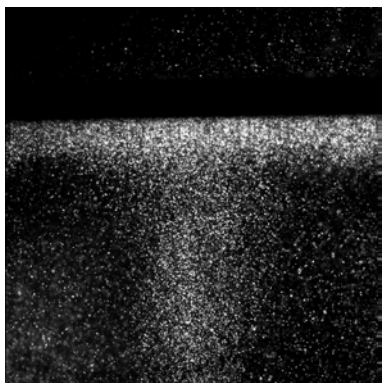

Fig. 3. Raw image of camera 2.

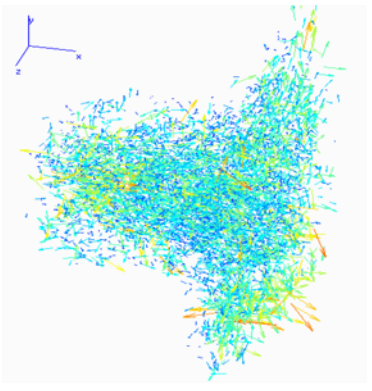

Fig. 4. Instantaneous vectors with error vectors.

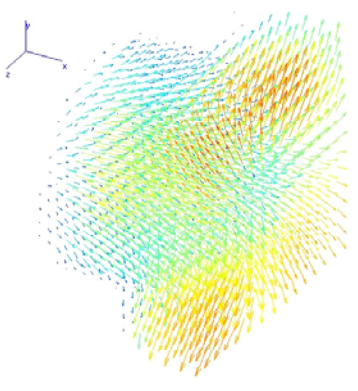

Fig. 5. Ensemble averaged grid vectors.

According to the report made by Kataoka et al. (1986), it is known that the periodical vortex series can change the effect of heat transfer at the impinged plate after observing a large period vortex on the round nozzle jet. This fact can be explained by the series of vortical structures as seen in Fig. 6 and Fig. 7. In order to make out characteristic structures of the vortices, an eigenvalue analysis method (λ_2 method, Jeong and Hussain, 1995) was introduced. The instantaneous three-dimensional velocity vectors on grids obtained by the 4D-PTV system can be formulated into

velocity gradient tensor ($\nabla\vec{u} = u_{i,j}$, vorticity tensor) and the characteristic equation can be approximated with the Taylor series expansion expressed as following Eq. (6). The eigenvalues, σ , of $\nabla\vec{u}$ satisfy the Eq. (6).

$$\sigma^3 - P\sigma^2 + Q\sigma - R = 0,\ P = u_{i,j},\ Q = \frac{1}{2}\left(u_{i,j}^2 - u_{i,j}u_{j,i}\right),\ R = Det\left(u_{i,j}\right) \tag{6}$$

The vortex core exists when the solutions of this equation have complex numbers, which implies that the vortex core can be found when the sign of the discriminant equation Eq. (7) is positive.

$$\Delta = \left(\frac{1}{3}Q\right)^3 + \left(\frac{1}{2}Q\right)^3 > 0 \tag{7}$$

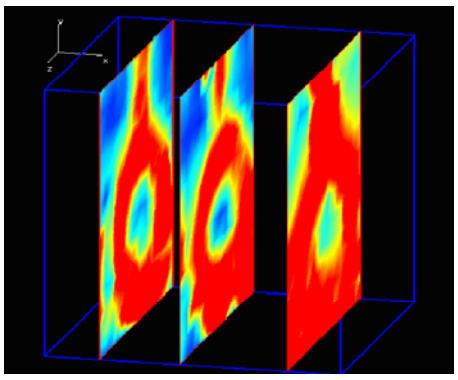

Fig. 6. Instantaneous vorticity distribution on YZ planes at x/D = 2.3, 3,5 and 5.1.

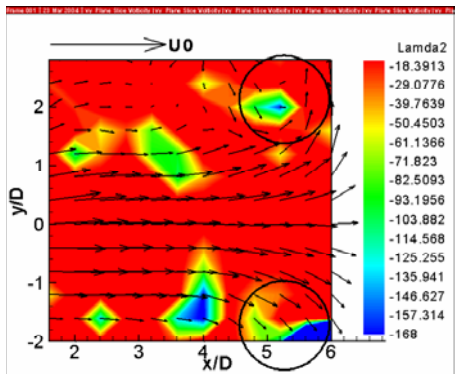

Fig. 7. Instantaneous vorticity distribution on XY center plane.

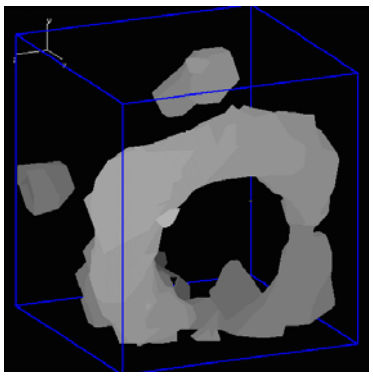

Fig. 8. Vortex loop obtained by 4D-PTV.

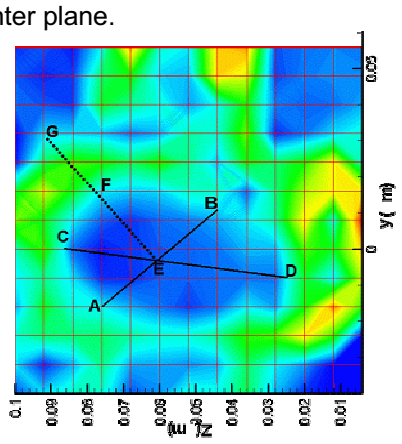

Fig. 9. Topology of the vortex loop.

Since the impinged jet flow field is very complicated, complex numbers exist over the whole flow field, and it is not so easy to find out conspicuous flow structures. In order to make a quantitative analysis on most conspicuous vortical structures, a new characteristic equation was formulated with a new tensor A_{ij} consisting of symmetric (S_{ij}) and asymmetric (R_{ij}) tensors defined as Eq. (8) (i.e., $A_{i,j} = S_{i,j}S_{i,j} + R_{i,j}R_{i,j}$) with which the solutions of the new equation become real numbers, which makes a quantitative evaluation.

$$S_{i,j} = \frac{1}{2}\left(u_{i,j} + u_{j,i}\right),\ R_{i,j} = \frac{1}{2}\left(u_{i,j} - u_{j,i}\right) \tag{8}$$

Figure 8 shows the vortical structure when the solutions (or eigenvalue) of the new characteristic equation are the second biggest value among the eigenvalues. It can be said that a large vortex loop exists near the impinged plate. Figure 9 represents the cross section of the ring vortex obtained at another instance. It showed that the location of the center of the vortex loop was close to 0.9D from the plate. It also showed that the thickness of the vortex loop was about 0.8D (line of FG). The inner diameter of the loop was 1.8D (line of AB). According to the study of Astarita et al. (2001), the

minimum and maximum in heat transfer coefficients are seen at r/D = 1.3 and r/D = 2.2, implying the thickness of the ring vortex is 0.9D(= 2.2D – 1.3D) and this value is very similar to 0.8D obtained in this study. The topological results obtained by the constructed 4D-PTV support well this fact.

Figure 10 shows the temporal evolution of the results measured for 250 consecutive image frames at x/D = 5.9, y/D = 1.4, z/D = -0.1. The time step is 0.5 msec (= 1/2000 frames/sec).

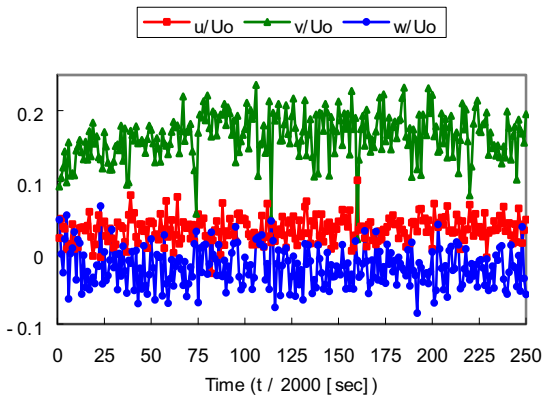

Fig.10. Temporal evolution of velocity components (at x/D = 5.9, y/D = 1.4, z/D = -0.1, step = 0.5 msec).

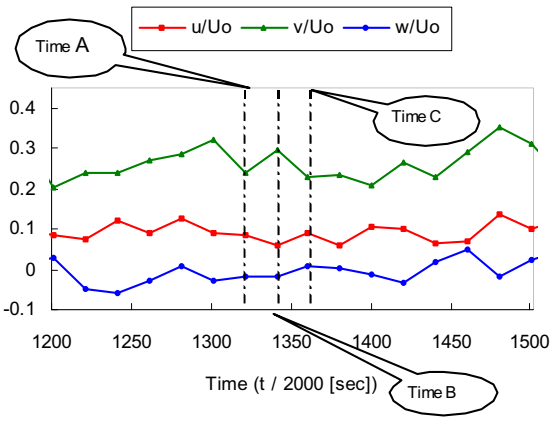

Fig. 11. Temporal evolution of velocity components (at x/D = 5.8, y/D = 2.4, z/D = 0, step = 10 msec).

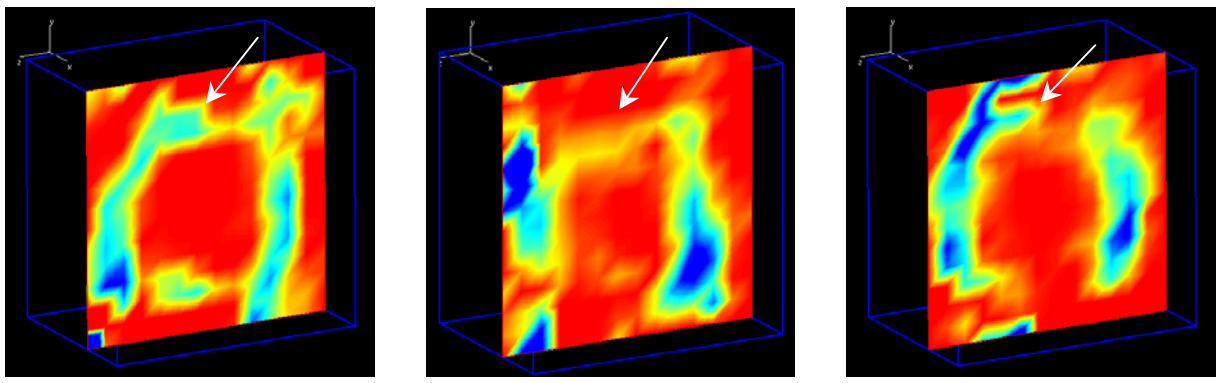

(a) at Time A = 1321/2000 sec (b) at Time B = 1341/2000 sec (c) at Time C = 1361/2000 sec

Fig. 12. Temporal changes of the vortex ring structures sampled at the times figured on Fig. 11.

v/Uo profiles show periodical peaks as indicated in the figure fluctuating near 0.15 with time evolution while u/Uo and w/Uo components show stationary random fluctuation near zero. This explicitly supports the existence of a strong ring vortex in front of the plate. Here, Uo means the average velocity of the jet nozzle. The average time difference between the conspicuous peaks (peak to peak) of v/Uo component was about 40/2000 sec. It can be said that this time interval corresponds to the passing interval of the ring vortices over the surface of the impinged plate. Figure 11 shows the temporal changes of the velocity components at x/D = 5.8, y/D = 2.4, z/D = 0 ranging from 1250/2000 ~ 1500/2000 sec. The data were sampled with 20/2000 sec time interval corresponding to half value of 40/2000 sec in order to investigate the states of the ring vortex at the instances of the two peaks and at the middle instance between the two peaks. It can instinctively be said that the structure of the ring vortex at the Time A and Time C would be similar each other while the structure at the Time B would be a topologically different one. Surprisingly, two conspicuous structures were seen at Time A (=C) and Time B as expected as shown in Fig. 12. The velocity components of Fig. 11 were sampled at the position indicated with a white arrow. These figures show the cross-sectional structures of the ring vortex at the instances of 1321/2000 sec, 1341/2000 sec and 1361/2000 sec. It can be said that the appearance of the two structures with some time interval implies that the vortex ring are “squeezed

in horizontal and in vertical with some interval" due to the vortex interactions between the smaller vortices embedded in the ring vortex.

4. Conclusion

4D-PTV technique was constructed through an experiment on an impinged jet using high-speed-high-definition cameras. More than 5000 instantaneous correct vectors were able to be measured by the system.

The ring vortex was clearly reconstructed by the obtained velocity vectors through an eigenvalue analysis. The location of the ring vortex, 0.9D from the plate, was at reasonable positions which were confirmed by previous research results. And the thickness of the ring vortex was about 0.8D. The results showed that the sweeping velocity of the ring vortex over the surface of the impinged plate was about 20 msec. It seems that the ring vortex appears periodically and shows a squeezing motion in horizontal and in vertical with some intervals.

The results obtained in the experiment of the impinged jet imply that the system not only makes possible to obtain the temporal evolution of turbulence properties but also makes possible to capture the instantaneous flow structures.

To use the 4D-PTV system for higher turbulences, the least sampling frequency of the system should be higher than that of the flow fields. The time scale of the smallest eddies in the turbulent flow field is represented with a Kolomogorov time scale $\tau = (\nu/\varepsilon)^{1/2}$. The maximum value of the viscous dissipation (ε) in this experiment is about 0.0075 m^2/s^3 from which the time scale is estimated as τ = 0.012 s (12 ms) with $\nu = 1 \times 10^{-6}$ m^2/s. It is apparent that the time interval between image frame, Δt = 0.5 ms which is shorter enough than the Kolomogorov time scale. The Kolomogorov length scale estimated is $\eta = (\nu^3/\varepsilon)^{1/4}$ = 0.11 mm. The cell size for data processing in this case is 3.3 mm and it is still too large to resolve the smallest eddies. However, it is noted that the purpose of the study is to construct a time-resolved 3D-PTV system and to show temporal evolution of the major flow structure, the ring vortex. Overcoming the spatial resolution of the system can be attained by reducing the measurement size only, which makes detailed investigations on smaller flow structures.

Acknowledgements

This work was carried out as parts of the BK21 Project of Ministry of Education of Korea and was partly supported by Korea Research Foundation Grant (KRF-2004-002-D00082). The authors express sincere thanks to Dr. M. Ishikawa of Tokyo Univ. for his helps for the experiments.

References

Astarita, T., Cardone, G. and Meola, C., Fluid Dynamics in an Impinging Air Jet, Proc. of 4th International Symposium on Particle Image Velocimetry,(Göttingen, Germany), (2001), Paper No. 1015.

Bae, S. T., Kim, D. K. and Kim, S. B., An Experimental Study on Flow Characteristics of Impinging Jet, Journal of the Korean Society of Marine Engineers, 25-2 (2001), 173-179.

Burmeister, L. C., Convective Heat Transfer, (1983), Wiley, New York.

Coleman, H. W. and Steele, W. G., Experimentation and Uncertainty Analysis for Engineers (2nd Ed.), (1999), 257-269, A Wiley-Interscience Publication.

Doh, D. H., Kim, D. H., Cho, K. R., Cho, Y. B., Saga, T. and Kobayashi, T., Development of GA based 3D-PTV Technique, Journal of Visualization, 5-3 (2002), 243-254.

Doh, D. H., Hwang, T. G. and Saga, T., 3D-PTV Measurements of the Wake of a Sphere, Measurement Science and Technology, 15-6 (2004), 1059-1066.

Faggiani, S. and Grassi, W., Impinging Liquid Jets on Heated Surfaces, Proc. of the 9th International Heat Transfer Conference, 1 (1990), 275-285.

Gardon, R. and Akfrat, J. C., The Role of Turbulence in Determining the Transfer Characteristics of Impinging Jet. Int. J. Heat Mass Transfer, 8 (1965), 1261-1272.

Hagiwara, Y., Nishino, M., Tanaka, M. and Skamoto, S., 3D-PTV Measurement on Turbulence Modification due to Oil Droplet in a Plane Couette Water Flow, Journal of Visualization, 3-3 (2000), 101-114.

Jeong, J. and Hussain, F., On the Identification of a Vortex, Journal of Fluid Mechanics, 285 (1995), 69.

Kataoka, K., Mihata, I., Maruo, K., Suguro, M. and Chigusa, T., Quasi Periodic Large Scale Structure Responsible for the Selective Enhancement of Impinging Jet Heat Transfer, Proc. of the 8th Int. Heat Transfer Conf., 3 (1986), 1193-1198.

Mass, H. G., Gruen, A. and Papantoniou, D. A., Particle Tracking Velocimetry in Three-dimensional Flows, Part 1

Photogrammetric Determination of Particle Coordinates, Exp. in Fluids, 15 (1993), 133-146.
Nishino, K., Samada, M., Kasuya, K. and Torii, K., Turbulence Statistics in the Stagnation Region of an Axisymmetric Impinging Jet Flow, Int. J. Heat and Fluid Flow, 17 (1996), 193-201.
Nishino, K. and Takahashi, T., High-speed PIV Applied to a Submerged Circular Impinging Jet, Proc. 5th International Symposium on PIV (PIV'03) (Busan, Korea), (2003), Paper No.3217.
Olsson, R. G. and Turkdogan, E. T., Radial Spread of a Liquid Stream on a Horizontal Plate, Nature, 211 (1966), 813-816.
Sibulkin, M., Heat Transfer near the Forward Stagnation Point of a Body Revolution, Journal of the Aeronautical Sciences, 9 (1952), 570-571.
Vader, D. T., Incropera, F. P. and Visskanta, R., Local Convective Heat Transfer from Heat Surface to an Impinging Planar Jet of Water, International Journal of Heat and Mass Transfer, 34-3 (1991), 611-623.

Author Profile

Tae Gyu Hwang : He received a B.A at Korea Maritime University (KMU) in 2001. He finished his M.Sc. degree at KMU in 2003. He is a Ph.D candidate of mechanical engineering at KMU since 2003. His recent research area is on the near wake of a sphere using 3D PTV and on an impinging jet flow using 4D-PTV technique. His research interests are thermal flow visualization using 3D-PIV, 3D-PTV and micro PIV techniques.

Deog Hee Doh: He received B.A. at Korea Maritime University (KMU) (1985). He finished his M.Sc. degree at the graduate school of KMU(1988). He received his Ph.D. degree at the Department of Mechanical Engineering of the University of Tokyo, Japan in 1995. His graduate works is on the development of 3D-PTV and simultaneous measurement techniques on temperature and velocity fields for thermal flows. He worked as an invited researcher for the Advanced Fluid Engineering Research Center (AFERC) in 1995. He has been working for Korea Maritime University since 1995 at the School of Mechanical and Information Engineering. His research subjects are to develop spatial measurement techniques such as 3D-PIVs, 3D-PTVs for the analysis of turbulent flows.

Koji Okamoto: He received his M.Sc.(Eng) in Nuclear Engineering in 1985 from University of Tokyo. He also received his Ph.D. in Nuclear Engineering in 1992 from University of Tokyo. He worked in Department of Nuclear Engineering, Texas A & M University as a visiting associate professor in 1994. He works in Nuclear Engineering Research Laboratory, University of Tokyo as an associate professor since 1993. His research interests are Quantitative Visualization, PIV, Holographic PIV Flow Induced Vibration and Thermal-hydraulics in Nuclear Power Plant.